

## Landscape resource mapping for wildlife research using very high resolution satellite imagery

Mariano R. Recio<sup>1,2\*</sup>, Renaud Mathieu<sup>3</sup>, G. Brent Hall<sup>1</sup>, Antoni B. Moore<sup>1</sup> and Philip J. Seddon<sup>2</sup>

<sup>1</sup>School of Surveying, University of Otago, Box 56 Dunedin, New Zealand; <sup>2</sup>Department of Zoology, University of Otago, Box 56 Dunedin, New Zealand; and <sup>3</sup>Earth Observation Research Group, CSIR-Natural Resource Environment, Pretoria, South Africa

### Summary

1. Quantifying wildlife-habitat relationships through resource selection analysis (RSA) has traditionally relied on landscape variables extracted at medium-to-coarse scales and general-purpose digital maps. However, RSA at fine scales, facilitated by accurate positional data obtained using GPS-tags, requires improved measures of habitat resources. The combination of cutting-edge remote sensing technology, such as very high spatial resolution (VHSR) satellite imagery and object-based image analysis (OBIA), can provide landscape maps that are suitable for the extraction of detailed variables at fine scale.

2. We used Quickbird satellite imagery and OBIA to produce a map using the multispectral bands (MULT), and explored the usefulness of the technique for resource identification by combining the panchromatic (highest spatial resolution) and multispectral (spectral information) bands (PAN:MULT) to produce a second map. Each of the mapping methods was used in a heterogeneous braided-river environment in New Zealand to: (1) classify and delimit ground features using an object-based accuracy assessment approach; (2) detect ground features of different sizes; (3) extract independent landscape variables at fine scale (within buffers between 20 and 30 m) for separate RSA for introduced hedgehogs (*Erinaceus europaeus*) and feral cats (*Felis catus*).

3. Per-pixel accuracy assessment produced overall accuracies of 82% (PAN:MULT) and 79% (MULT). The per-object assessment using shrubs as the testing class yielded further information on classification and delimitation of object accuracy, with accuracies of 80% for shrub patches  $\geq 30$  m<sup>2</sup> in MULT and  $\geq 5$  m<sup>2</sup> in PAN:MULT. The inclusion of the panchromatic band noticeably improved the identification and delimitation of cover. However, RSA using each of the maps did not yield differences in the best models for cats or hedgehogs.

4. VHSR imagery and OBIA provide a valuable method to identify smaller ground features and thus to produce more detailed landscape maps to study animal habitat use at fine scale. Improvements in ground feature detection achieved by including the panchromatic band may not justify its cost, as it was shown for the studies on cats and hedgehogs presented here. However, the level of detail offered by the panchromatic layer may be useful for addressing other RSA questions or applications at fine scale, such as remote censusing of colonial species.

**Key-words:** fine scale, object-based image analysis, Quickbird, resource selection, very high spatial resolution, wildlife research

### Introduction

The collection of landscape variables to model wildlife-habitat relationships has traditionally relied on field surveys, aerial photographs (for on-screen digitizing of landscape features) or general-purpose digital land-cover maps derived from pixel-based classification of medium resolution satellite imagery (e.g. Landsat) (Estes *et al.* 2010; Lahoz-Monfort *et al.* 2010). One area of wildlife research that has most benefited from digital land-cover maps is resource selection analysis (RSA), which enables quantification and estimation of animal space-use conditioned by the occurrence of a set of environmental variables (Forester, Im & Rathouz 2009; Franklin 2010). RSA can be

based either on the identification of disproportionate use of certain habitats in relation to their occurrence, or on the probability of obtaining an animal relocation within a specific habitat (Moorcroft & Barnett 2008). Methods for RSA include: resource selection functions (RSFs) based on the comparison of used and available locations and their associated resources using logistic regression (Boyce & McDonald 1999), resource utilization functions (RUFs) based on modelling of resource use as a probabilistic use of space (Marzluff *et al.* 2004), and step selection functions and mechanistic models based on resource use in terms of underlying patterns of animal movement (Forester, Im & Rathouz 2009).

Resource selection occurs at hierarchical nested scales, and thus, the full ecological context of wildlife-habitat relationships can be characterized using multiscale modelling (Boyce 2006). Animal ecology research has entered a period of rapid

\*Corresponding author. E-mail: mariano.recio@otago.ac.nz

advances through the application of global positioning system (GPS) technology for wildlife tracking, providing accurate and abundant animal location data suitable for studying individual movements and behavioural processes at fine scale (Recio 2011). However, fine-scale RSA, either stand-alone or within the context of a multiscale method, requires spatially detailed quantification of resources, since fine-scale resource selection by animals varies according to fine-scale resource availability patterns (Mysterud & Ims 1998). Thus, in order to address resource selection hypotheses at a fine scale, accurate animal location data must be matched with similar quality measures of resource availability (Hebblewhite & Haydon 2010). Consequently, fine-scale measures of land-cover require a method that is small grain (the minimal distinguishable element contained in a spatial data set) and small extent (the area encompassed by the data source). Specific landscape composition and configuration at local sites can be relevant for local processes and behaviour, including characterization of nesting or denning sites, the identification of fine-scale movement pathways, or the specific use of small localized sites, such as for ectothermic species' thermoregulation (Rubio & Carrascal 1994).

Currently, very high spatial resolution (VHSR) satellite imagery approaches the spatial resolution of aerial photography and also provides spectral bands suitable for vegetation characterization, for example infrared bands (Chuvieco 2006). Commercial satellites, such as IKONOS, Quickbird, Pleiades-HR or GeoEye-1, deliver multispectral (blue, green, red and near infrared –NIR–) and panchromatic (single black and white) bands with resolutions below 4 and 1 m, respectively. The detection of ground objects can be enhanced by combining the benefits of panchromatic (higher spatial detail) and multispectral (improved spectral information) bands through physically based image fusion or pansharpening (Pohl & van Genderen 1998), or the use of analytical methods capable of integrating the two data sets within a common processing framework, for example object-based imagery analysis (OBIA) (Blaschke 2010). One advantage of OBIA techniques over pixel-based classification methods is that the image classification process approximates that of human perception by segmenting the image into 'image objects' (groups of contiguous pixels). These groups can be then assigned to an object class using a range of object features describing spectral, textural, morphological, topological and contextual properties (Benz *et al.* 2004). This capacity to delineate coherent ground features at different scales provides an appropriate representation of meaningful patches or ecological entities (Addink, de Jong & Pebesma 2007; Chen *et al.* 2011).

Research is required to assess the applicability of VHSR and OBIA techniques for extracting land-cover information necessary for hypotheses on wildlife research at fine scale and to assess whether the increased cost of using panchromatic data is justified by improvements in ground feature detection (Horning *et al.* 2010). To examine this question, we applied VHSR and OBIA techniques to produce land-cover maps for use in RSA of feral cats (*Felis catus*) and hedgehogs (*Erinaceus europaeus*) in braided-river environments of New Zealand

(NZ). Both predators pose a threat to native species; hence, an understanding of resource selection at a fine-scale is, *inter alia*, important to guide trap placement to maximize capture rates and to minimize logistic effort and costs (Cameron *et al.* 2005).

Our objectives are to combine remote sensing technology, VHSR satellite imagery and OBIA to produce resource maps suitable for extracting landscape composition and configuration patterns required for wildlife spatial analyses at a fine scale; to measure the extra accuracy gained through the incorporation of the higher resolution panchromatic layer (hereafter PAN:MULT) relative to the multispectral data set only (MULT) in the classification process; and to assess the performance of each map in deriving RSFs for feral cats and hedgehogs. RSF was selected because it is an accurate and widely used RSA method applied for quantifying habitat selection by animals using radiotracking and GPS-tracking data.

## Materials and methods

### STUDY AREA

The research area covers 166.97 km<sup>2</sup> in the braided-river environment of the Godley Valley, South Island, NZ (Fig. 1), where predation by feral cats and hedgehogs poses a risk to endemic ground-nesting birds such as the critically endangered black stilt (*Himantopus novaezelandiae*) (IUCN 2012). This typical 'U'-shaped valley is a consequence of glaciation cycles, with a valley floor dominated by free-draining gravels and braided-river channels bounded by steep mountain slopes. Elevation ranges between 710 and 2420 m, with average slopes of 14 ± 22% (Mean ± Standard deviation) and a maximum of 82%.

Vegetation on the floodplain ranges from active river channels where little or no vegetation occurs, to terraces and low mountain slopes with diverse vegetation communities, including patchy matagouri shrubs (*Discaria toumatou*) and sparse exotic sweet briar (*Rosa rubiginosa*), improved and unimproved pastures, sparse native short tussocks (e.g. fescue tussock, *Festuca novaezealandiae* and silver tussock *Poa cita*), scattered tall tussocks (*Chionochloa* spp.) and herbs. Shrubs are replaced by dry tussockland at higher altitudes, and screes are common on mountain slopes. Sparse patches of exotic tree species such as conifers, willow (*Salix* spp.) and birch (*Betula* spp.) also occur.

Landscapes combining grasslands with patches of sparse individual shrubs and/or shrub aggregations at lower elevations are reported to be the most suitable for introduced rabbits (*Oryctolagus cuniculus*), the staple prey of cats in braided-river environments and a major determinant of cat presence (Gillies 2001; Recio 2011). Mosaics of grasslands and shrubs also provide numerous transitional edges relevant for hedgehog movements (Recio 2011; Recio *et al.* 2013). Shrubs are a critical resource for hedgehogs and feral cats in braided-river environments because they provide shelter, protection (hedgehog nests are usually made underneath shrub clumps, Jones & Norbury 2006) and refugia (Gillies 2001). Accurate quantification at fine scale of habitat classes and landscape indices is necessary in this heterogeneous environment where species select specific landscape patterns at local sites.

### DATA AND IMAGE PREPROCESSING

A panchromatic and multispectral Quickbird image bundle (0.6 m and 2.4 m spatial resolution, respectively) was acquired to elevations

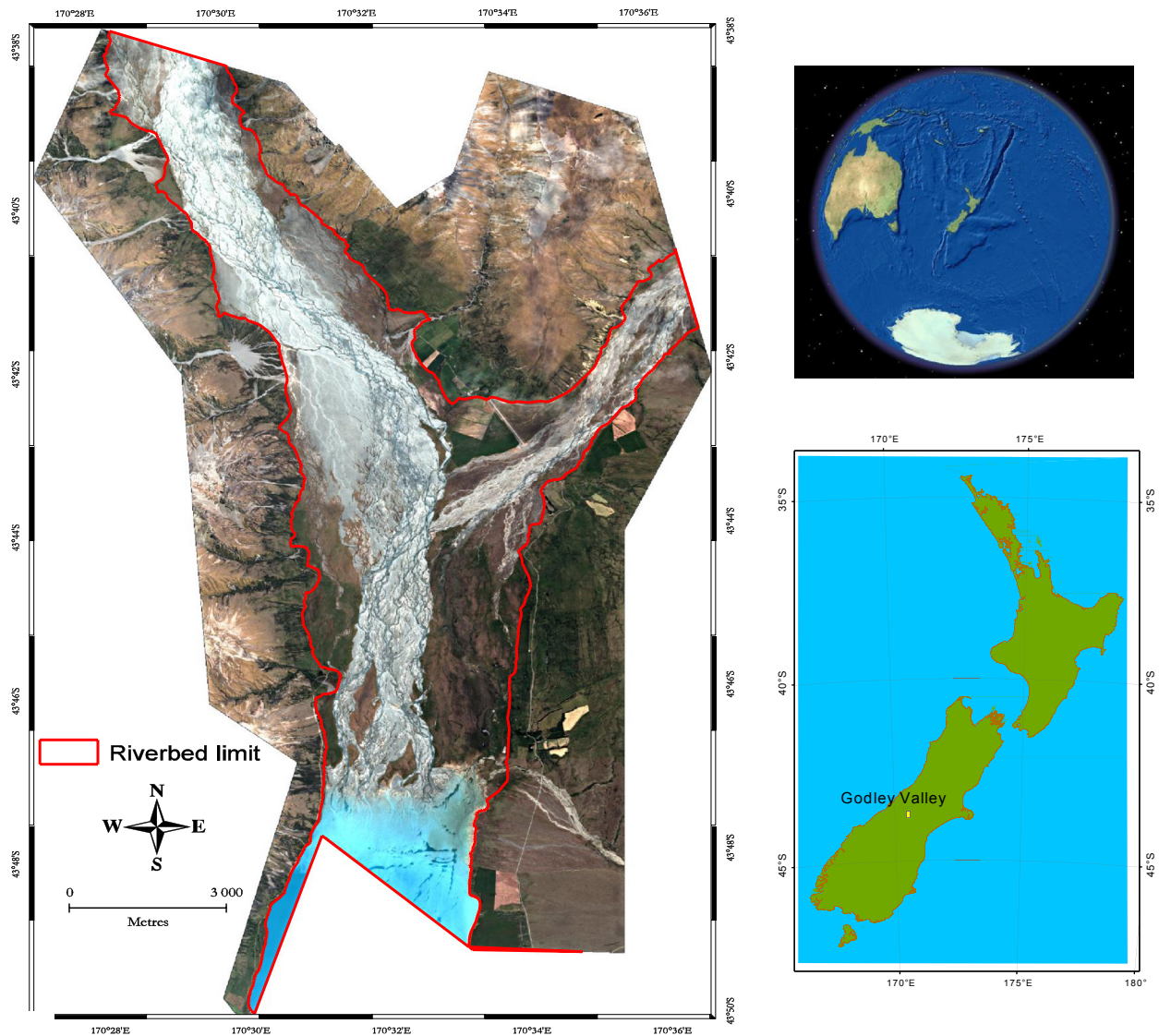


Fig. 1. Quickbird multispectral image of the Godley Valley, and its location in the New Zealand South Island.

between 710 and 2000 m A.S.L. (Fig. 1). We orthorectified the images with ERDAS Imagine 9.3 software using a 15 m digital elevation model (DEM) and a second-order refinement of the rational polynomial coefficient (RPC) provided by the image provider (Toutin 2004). The DEM was produced using 1:50 000 vector topographic maps from Land Information New Zealand (LINZ). A total of 66 ground control points were surveyed on-site using a differential GPS Leica® GS20. One-third of these were used as control points (25 points, model production) and two-thirds as checkpoints (41 points, model validation). Orthorectification yielded average root-mean-square error (RMSE) values of 0.78 m and 0.63 m in the horizontal (x) and vertical (y) directions, respectively, with maximum RMSE values of 1.2 m and 1.25 m.

We corrected the imagery for atmospheric and topographic distortion using the ATCOR3 package (Richter 1998) included in PCI Geomatics 9.1 software (PCI Geomatics Enterprises Inc.). This was used to calculate ground equivalent reflectance by minimizing the atmospheric (water vapour, aerosols) and illumination effects (considering ground elevation and sensor–target–sun geometry). Three parameters were required in ATCOR3 including ground visibility, adjacency neighbourhood and sensor-viewing angle (Richter 1998). The ground visibility was set to 50 km, as provided by the National Climate Database

([www.cliflo.niwa.co.nz](http://www.cliflo.niwa.co.nz), accessed 20 July 2013), for the area and the date when the image was taken. The adjacency neighbourhood was set at 500 m to define the distance up to which nearby targets influence the reflectance measured for a given pixel as a result of multiple atmospheric scatterings. The sensor-viewing angle for the image was 10° west.

#### CLASSIFICATION METHODS

Nineteen nonvegetation and vegetation classes were mapped considering their likely discrimination in the scene and their relevance as resources for introduced predators. Nonvegetation classes included gravel/stones, bare soil on slopes, fine soil, rivers, lakes/lagoons/ponds, roads, tracks, buildings, snow and shadow. Vegetation classes included sparse barren rock vegetation, brown meadow, mixed meadow, green meadow, shrubs, conifers, deciduous trees, crops and wetlands (see Table S1, Supporting information for class descriptions). Grasslands and shrublands are the most abundant vegetation classes in the study area. The shrub class is patchy, and thus, mapping of shrubs at clump or individual level was required to provide reliable fine-scale information on landscape composition and configuration. The spectral

signatures of dominant shrubs in the area (i.e. matagouri and sweet briar) were very dark and contrasted well with the much brighter or greener grasslands. This contrast was captured well in the 0.6 m panchromatic layer which, combined with the coarser multispectral image (2.4 m), facilitated the detailed delimitation and extraction of shrub cover (Laliberte *et al.* 2004). Grasslands were included in three different meadow classes according to their level of greenness (or photosynthetic activity), ranging from tussocklands characterized by a typical brown colour, to exotic green meadows used by livestock.

An OBIA classification using eCognition Developer™ 8.0.1 software (Definiens 2010) produced two maps, one using the multispectral bands only (MULT) and the other using both the multispectral and panchromatic bands (PAN:MULT). eCognition allows for the simultaneous inclusion of spectral bands with different spatial resolution to take advantage of both fine spatial resolution (panchromatic) and high spectral resolution (multispectral). The image was then segmented and classified (see Fig. 2 and Table S2, Supporting information).

Segmentation subdivided the image into image objects or primitives (approximating ground targets, e.g. shrub patch) by clustering pixels into contiguous regions of minimum heterogeneity at a given scale (Benz *et al.* 2004). We applied a  $3 \times 3$  low pass filter to the panchromatic image before segmentation to reduce noise effects and ancillary vector layers, such as lakes, river floodplains, tributary streams, tracks, roads and wetlands, were used in the segmentation process to maintain the integrity of the boundaries of these features. A multiresolution segmentation was used to optimize the mapping of ground features characterized by a wide range of sizes and shapes, from small clumps of shrubs to large patches of forest or pasture.

The first segmentation (Level1) used a low scale parameter (scale = 5 for PAN:MULT and 15 for MULT) to delimit the smallest ground features. Segmentation at these scales tends to over-split medium-to-large ground features (e.g. large grass patches) into a large number of objects. Hence, we used a spectral difference segmentation to merge contiguous objects having similar mean reflectance values. Occasionally resulting objects extended beyond the boundaries of medium-to-large ground features; thus, we applied another segmentation (Level2) using a larger scale parameter (scale = 30 for PAN:MULT and 90 for MULT) (see Table S2, Supporting information for additional details on parameters used for the segmentation). The resulting Level2 objects were used as input for the classification process.

When classifying objects, eCognition uses object descriptors or 'features' to assign an object to a class using crisp or fuzzy transition functions, or by the application of nearest-neighbour membership functions trained by representative class samples (Benz *et al.* 2004; Definiens 2010). We applied both crisp rules and nearest-neighbour membership functions as shown in the classification flowchart in Fig. 2. For the latter, we selected between 10 and 20 object samples per class (depending on class abundance in the study area) as training references for the classification. The appropriate class for each training reference was determined from either field surveys or directly from the image. Four methods were considered for discriminating the land-cover classes in eCognition, namely (1) *statistical* (e.g. mean, standard deviation, ratios and minimum and maximum of pixel values within an object); (2) *textural* (e.g. mean difference to neighbours, Haralick indices); (3) *contextual descriptors* (e.g. mean difference of an object between inner and outer border or scene); (4) *spectral indices for vegetation and bare ground characterization*, such as the Soil-Adjusted Vegetation Index (SAVI) (Huete 1988), Hue, Saturation and Intensity indices, and blue index (blue index = blue/[green + red + NIR]). Some classes were visually interpreted and classified or derived from ancillary data (Fig. 2).

We assessed class separability and selected the best discriminating features using the feature space optimization tool in eCognition. This tool uses the training references to measure the statistical distance between classes for a set of features and displays a class separation distance matrix (Definiens 2010). A high separation distance between two classes suggests that the selected features can discriminate the two classes. SEATH\_GUI software (<http://tu-freiberg.de/fakult3/mage/geomonitoring/software/software.en.html>, accessed 25 March 2013) was also used to identify those features that separated classes using a Jeffries-Matusita distance measure (J) above 1.3 (J = 0 means complete correlation or low separability and J = 2 means complete noncorrelation and high separability). These features were retained and incorporated either in crisp membership functions or applied to a nearest-neighbour classifier (Fig. 2).

#### ACCURACY ASSESSMENT

Traditional methods used to assess classification accuracy have relied on per-pixel methods, where the correctness of a classification is assessed for a sample of single pixels or groups of pixels for each class under consideration (Zhan *et al.* 2005). When object-based techniques are used, a per-object assessment evaluates not only the thematic correctness (class matching) of objects, but also their geometric accuracy. This is generally achieved by comparing classified objects with reference objects delineated in the field using a GPS or directly on the image through on-screen digitizing (Möller, Lymburner & Volk 2007). However, the delimitation of reference objects can be challenging in a natural or semi-natural environment due to the fuzzy nature of natural boundaries. We carried out a per-pixel assessment (Congalton 1991) and a per-object assessment (Zhan *et al.* 2005; Mathieu, Freeman & Aryal 2007; Möller, Lymburner & Volk 2007) for each of the maps produced. Indices employed to assess the classification accuracies are summarized in Table 1 according to nomenclature used by Congalton (1991) and Zhan *et al.* (2005).

#### Per-pixel method

We randomly selected 545 ground reference points, separated by at least 200 m to reduce the possibility of spatial autocorrelation (Congalton 1991). These points were checked in the field or directly on the image for the most easily identifiable classes (e.g. water bodies). We calculated producer's, user's and overall accuracies, as well as the kappa indices for each map (Congalton 1991) (Table 1). The kappa indices, as summarized by Skidmore (1999), were used to determine the statistical significance of differences between maps:

$$Z_{\text{PAN:MULT, MULT}} = \frac{\kappa_{\text{PAN:MULT}} - \kappa_{\text{MULT}}}{\sqrt{\sigma_{\text{PAN:MULT}} + \sigma_{\text{MULT}}}}; \quad \text{eqn 1}$$

where  $\kappa$  is the estimated kappa value and  $\sigma$  the variance of  $\kappa$  where the null hypothesis is rejected ( $H_0: \kappa_{\text{PAN:MULT}} = \kappa_{\text{MULT}}$ ) using the normally distributed  $z$  statistic via a two-tailed  $Z$ -test for  $\alpha = 0.05$  ( $z_t = 1.96$ ) if  $Z_{\text{PAN:MULT, MULT}} \Rightarrow z_t = 1.96$ .

#### Per-object method

We used the per-object assessment method proposed by Zhan *et al.* (2005) and Mathieu, Freeman & Aryal (2007), and focused on the assessment of the 'shrub' class due to its ecological relevance and because this class exhibits the highest level of fine-scale heterogeneity and patchiness in the study area. Moreover, shrub clumps contrast well

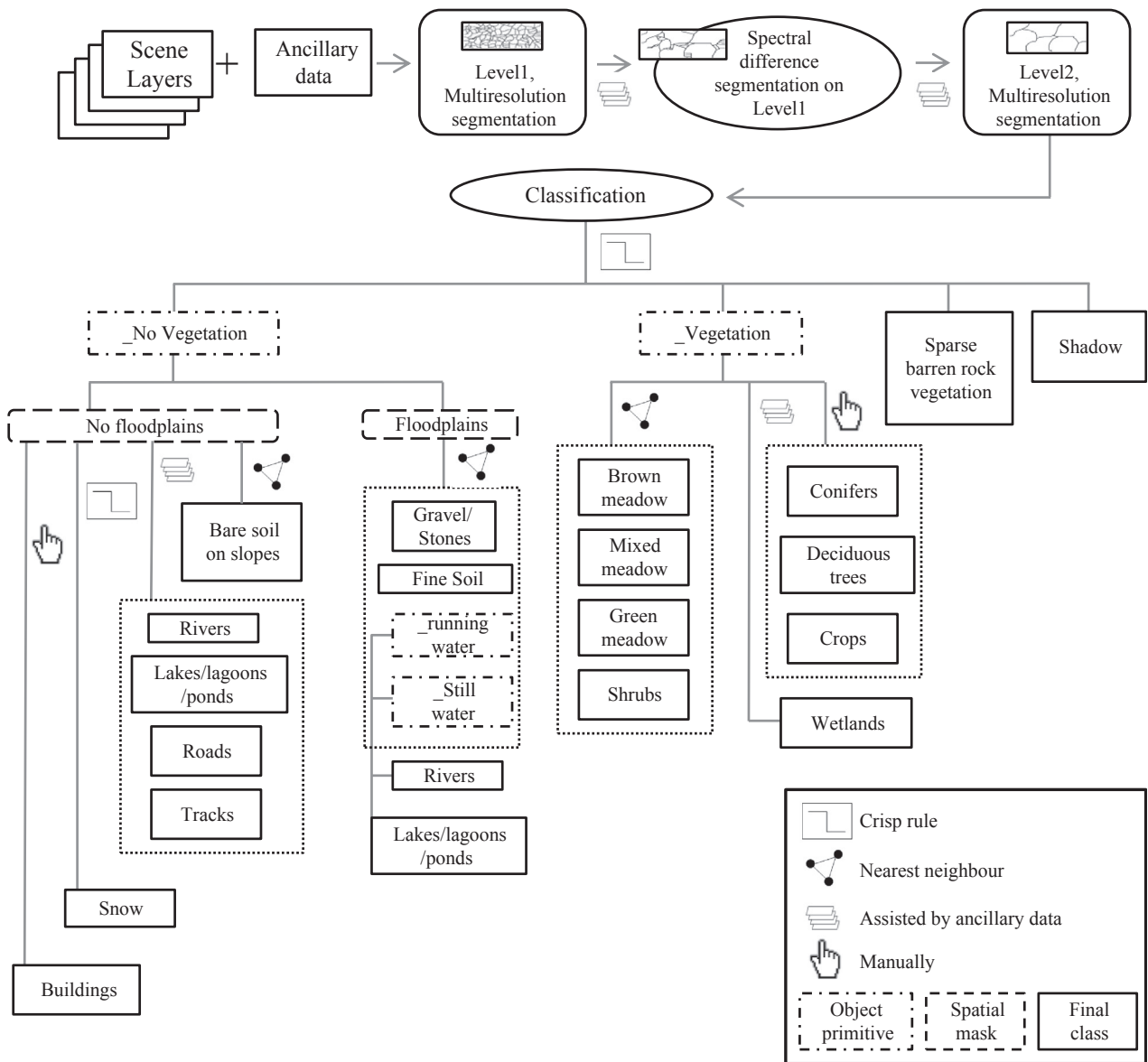


Fig. 2. Quickbird image classification workflow using eCognition Developer™ 8.0.1 software.

with surrounding targets, which makes it possible to delineate shrub reference objects with an acceptable accuracy, allowing an assessment of the classification accuracy from a geometric perspective.

We first selected random points distributed over the study area using ArcGIS 9.3 software (ESRI, Redlands, CA). Next, various shrubby scenarios were considered, and 45 representative points were selected located in either large patches of homogeneous shrub surfaces, clustered medium-size shrub patches or areas with encroachment of shrub clumps. Finally, a buffer of 30 m diameter was created around each selected point. A total of 1320 reference polygons or objects (hereafter referred to reference objects), representing individual shrubs or shrub patches between 0.36 m<sup>2</sup> and 3045 m<sup>2</sup>, were manually photo-interpreted and digitized from the panchromatic and multispectral data within the buffers. All targets included within the buffers, but not constituting shrub reference objects, were considered as a single 'no shrub' class (Fig. 3b). MULT and PAN:MULT classifications were reclassified as 'shrub' and 'no shrub' (hereafter referred to as classified objects) and compared to the reference objects.

The accuracy of the object-based method was assessed according to both the number of reference objects and the area of reference objects correctly classified as shrubs. We calculated the map accuracy as the common extent between the shrubs that had been photo-interpreted (reference data) and the shrubs classified in the Quickbird image. This assessment quantifies the level of mismatch between the reference and classified data.

The influence of the size of the reference objects on their detection (i.e. correct classification) was assessed in the MULT and PAN:MULT classifications (Zhan *et al.* 2005; Mathieu, Freeman & Aryal 2007; Möller, Lyburner & Volk 2007). Progressively, we removed the smallest objects from the reference data set, then re-assessed and compared the classification accuracy obtained after each object removal. We considered the removal of objects between 2 m<sup>2</sup> (expected smallest detectable shrub clumps with the panchromatic image) and 900 m<sup>2</sup> (equivalent to the 30 × 30 m Landsat pixel size) iteratively using the following size thresholds for object removal: below 2, 5, 10, 20, 30, 40, 100, 500 and 900 m<sup>2</sup>.

**Table 1.** Metrics used for classification accuracy assessment; after Congalton (1991) and Zhan *et al.* (2005)

Index			
Per-pixel	Per-object	Simplified formula	Description
Producer's accuracy	Completeness	$\frac{\text{\# of pixels or objects correctly classified as class } m}{\text{\# of ground reference pixels or objects of class } m}$	Probability that a reference pixel or object of class <i>m</i> in the image is correctly classified
User's accuracy	Correctness	$\frac{\text{\# of pixels or objects classified in class } m}{\text{total \# of pixels or objects classified in class } m}$	Probability that a pixel or object in the map corresponds to the feature on the ground
Overall accuracy	Overall accuracy	$\frac{\text{\# of pixels or objects correctly classified}}{\text{total \# of pixels or objects}}$	Overall probability that any pixel or object in the classified image has been correctly classified
Kappa index		$\frac{\text{observed accuracy} - \text{chance agreement}}{1 - \text{chance agreement}}$	Overall accuracy index to test the actual agreement and the agreement expected by chance

APPLICATION OF MAPS IN RESOURCE SELECTION FUNCTIONS

We assessed whether the inclusion of the panchromatic band provided additional information for RSAs modelled for feral cats and for hedgehogs tracked in the study area. For each species, we compared the best models obtained independently after using landscape variables extracted, respectively, from the MULT and PAN:MULT maps. To comply with a design II RSF (i.e. where an animal chooses to establish its home-range within the study area) (Boyce & McDonald 1999), we extracted variables relating to land-cover patterns within a 30 m radius buffer for cats and 20 m for hedgehogs around animal locations obtained by GPS-tracking (used) and around random points selected over the study area (available) (Recio 2011; Recio *et al.* 2013). These variables included shrubs, meadows, fine soils, gravel and stones on riverbed, crops, trees (deciduous and conifers), wetlands, distance to roads, tracks, fences and buildings, and total edge for both hedgehogs and cats; bare ground on slopes, elevation, aspect, slope, still water, rivers and distance to riverbed only for cats; and the normalized difference vegetation index (NDVI) (Tucker 1979) only for hedgehogs. Buffer sizes were set according to the estimated GPS locational accuracy and to approximate animal perceptions of their immediate surroundings (Recio *et al.* 2011, 2013).

Models representing alternative hypotheses were analysed as logistic regressions within a generalized linear mixed model (GLMM) framework (Hosmer & Lemeshow 2000), wherein the dependent variable took values 1 (used locations represented by GPS-tracking data) or 0 (available locations represented by random points over the study area) (Boyce & McDonald (1999). Best explanatory model was selected using Akaike Information Criteria (AIC) for model selection (Burnham & Anderson 2002). Further details of RSF can be found in Boyce & McDonald (1999), Recio (2011) and Recio *et al.* (2013).

Results

ACCURACY ASSESSMENT

Per-pixel method

Statistical results (producer's, user's and overall accuracies – see Table 1) for the per-pixel classification accuracy assessment

are shown in Table 2 (see also Tables S3–S4, Supporting information for full contingency matrices). The PAN:MULT overall accuracy was 82.9%, whereas MULT accuracy was slightly lower at 79.3%. Overall, the kappa analysis revealed that classification and reference data were in high agreement for both maps at the 95% confidence level (Table 2), with  $81.1\% \pm 3.2\%$  in PAN:MULT and  $76.9\% \pm 3.9\%$  in MULT.

Producer's and user's accuracies for the class 'shrubs' were over 75%. The producer's accuracy was significantly greater for PAN:MULT (90%) compared to MULT (75%), whereas user's accuracy was in a similar range for both PAN:MULT (76.6%) and MULT (78.9%). The lowest accuracy values were for the classes 'sparse barren rock vegetation' (SBRV), 'green meadow' and 'mixed meadow' in both maps, which suggested a need to merge these classes with 'brown meadow' to create a single class 'meadow'. This new class improved the overall classification to  $\pm 90\%$  in PAN:MULT and  $\pm 88.1\%$  in MULT. Comparison of per-pixel assessment results between PAN: MULT and MULT maps yielded no significant difference ( $Z_{\text{PAN:MULT, MULT}} = 1.61, z_{\alpha = 0.05} = 1.96$ ), before or after merging the above-mentioned classes ( $Z_{\text{PAN:MULT, MULT}} = 0.11, z_{\alpha = 0.05} = 1.96$ ).

Per-object method

Objects classified as shrubs in the Quickbird image typically encompassed multiple nearby shrub reference objects (Fig. 3). The PAN:MULT classification created a total of 455 shrub objects within the reference buffers. Thirty of these did not correspond to any shrub reference objects and 425 overlapped 792 shrub reference objects. The classification missed 528 shrub reference objects (Table 3). In contrast, the MULT classification created 133 shrub objects. Three of these did not correspond to any shrub reference object and 130 encompassed 444 shrub reference objects. Thus, 876 shrub reference objects were missed in the classification. The correctness (see Table 1) of the shrub class was high for both maps (93.4% PAN:MULT, 97.7% MULT), indicating that objects classified as shrubs

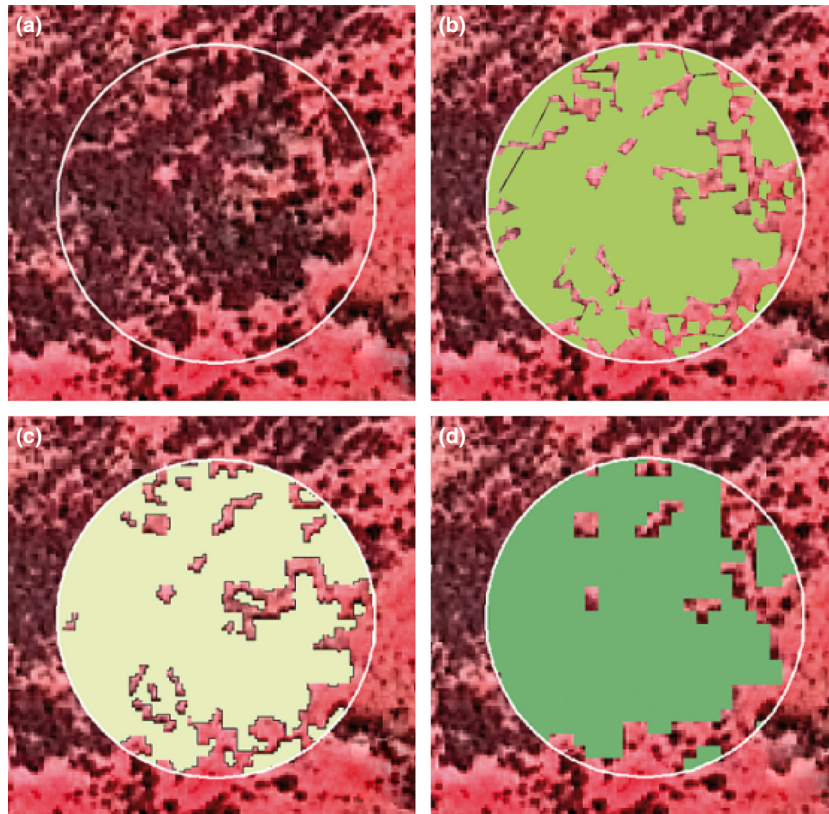


**Fig. 3.** Examples of object-based accuracy assessment of the class 'shrub' within selected buffers. (a) Raw buffer; (b) shrub objects manually digitized; (c) result of the shrub classification in the PAN:MULT map; (d) result of the shrub classification in the MULT map.

were indeed shrubs in the reference data set. However, the low completeness (Table 1) value for both methods (44.6% PAN:MULT, 12.9% MULT) indicates that a considerable number of shrub objects in the reference data set were incorrectly classified in the per-object approach.

The total area of objects classified as shrub was 63578.5 m<sup>2</sup> for PAN:MULT and 61461.5 m<sup>2</sup> for MULT. Both values were lower than the 70 610 m<sup>2</sup> of the shrub reference data and represented 90.0% and 87.0% of the reference cover area for PAN:MULT and MULT, respectively. The area overlap assessment between classified shrub objects and the reference revealed a correctness of 85.9% for PAN:MULT and 84.0% for MULT (Table 3), suggesting that most of the area detected as shrub was also shrub in the reference. Completeness was 77.3% for PAN:MULT and 73.1% for MULT, indicating that a relatively large area of reference shrubs was correctly classified as shrubs (Table 3).

The completeness accuracy increased sharply when the smallest shrub objects were removed from the reference data set (Fig. 4). The accuracy reaches a value close to or above 80% if only shrub reference objects larger than 5 m<sup>2</sup> for the PAN:MULT map and 30 m<sup>2</sup> for MULT are considered. This means, as expected, that larger objects have a higher probability of detection and that the higher spatial resolution of the panchromatic image enhances the ability to detect smaller objects. All shrub reference objects larger than 30 m<sup>2</sup> and 100 m<sup>2</sup> were detected, respectively, in the PAN:MULT and

MULT maps. In terms of area, the completeness accuracy also improved, albeit at a lower and more regular pace, as objects from 2 m<sup>2</sup> to 900 m<sup>2</sup> were successively removed (Fig. 5). Completeness increased from 77.3% to 85.9% in PAN:MULT and from 73.1% to 91.8% in MULT.

#### APPLICATION OF MAPS IN RSFS

Resource selection functions for feral cats and hedgehogs, using variables extracted from either the PAN:MULT or the MULT maps, yielded the same best models for both species. The best model for cats indicated that the species selected those sites with mixed shrubs, meadow and bare soils at low elevations (Table 4). Hedgehogs selected sites positively influenced by the amount of edge habitat, higher values of NDVI (i.e. high plant productivity) and areas closer to roads, but avoided areas close to tracks (Table 4). AIC values for all the best models obtained for both species were notably lower than those of the next rank showing little to no support for any of the alternative models tested.

#### Discussion

Collectively, our results suggest that the combination of VHSR satellite imagery and OBIA provides a powerful means to identify small ground features and is therefore suitable for the extraction of landscape variables to examine hypotheses

**Table 2.** Per-pixel classification accuracy metrics and statistics for the panchromatic and multispectral (PAN:MULT) and multispectral only (MULT) maps

Classes	PAN:MULT			MULT		
	Producer's (%)	User's (%)	Cond. $\kappa$ (%)	Producer's (%)	User's (%)	Cond. $\kappa$ (%)
Unclassified	NA	0.0	NA	NA	0.0	0
Fine soil	92.9	86.7	86.3 ± 17.9	71.4	76.9	76.3 ± 23.8
Gravel/stones	85.7	84.5	82.2 ± 9.6	88.6	82.7	80.1 ± 9.7
Rivers	83.3	71.4	70.4 ± 80.1	72.2	76.5	75.7 ± 21.1
Lakes/Lagoons/Ponds	76.9	100.0	100.0 ± 0.0	69.2	100.0	100.0 ± 0.0
Sparse barren rock vegetation	41.2	46.7	43.1 ± 18.8	38.2	50.0	46.7 ± 20.4
Brown meadow	89.0	80.8	76.0 ± 8.5	87.2	73.6	67.1 ± 8.9
Mixed meadow	62.3	71.7	68.7 ± 14.3	64.2	57.6	53.1 ± 13.5
Green meadow	57.1	57.1	56.0 ± 26.8	42.9	46.2	44.7 ± 28.0
Shrub	90.0	76.6	74.7 ± 13.0	75.0	78.9	77.3 ± 14.0
Conifers	90.9	90.9	90.7 ± 17.7	90.9	90.9	90.7 ± 17.7
Deciduous trees	81.8	100.0	100.0 ± 0.0	72.7	100.0	100 ± 0.0
Crops	95.0	100.0	100.0 ± 0.0	85.0	100.0	100 ± 0.0
Bare ground on slopes	96.8	90.9	90.4 ± 10.5	100.0	93.9	93.6 ± 8.8
Buildings	92.3	100.0	100 ± 0.0	76.9	100.0	100 ± 0.0
Roads	100.0	100.0	100 ± 0.0	81.8	100.0	100 ± 0.0
Tracks	70.0	100.0	100 ± 0.0	50.0	100.0	100 ± 0.0
Snow	90.9	100.0	100 ± 0.0	100.0	100.0	100 ± 0.0
Shadow	100.0	100.0	100 ± 0.0	100.0	100.0	100 ± 0.0
Wetlands	92.2	97.9	97.7 ± 4.5	94.1	96.0	95.6 ± 6.1
Overall accuracy (%)	82.9 ± 3.2			79.3 ± 3.5		
Kappa $\kappa$ (%)	81.1 ± 4			76.9 ± 3.9		

requiring fine-scale characterization of wildlife resources. The inclusion of the panchromatic band was shown to improve ground feature detection and delimitation. Classification assessment using the per-pixel method scored ‘almost perfect’ for the PAN:MULT map and ‘substantial’ for the MULT according to the Landis & Kock (1977) classification, becoming ‘almost perfect’ for both maps after merging classes into a new meadow class. Per-object accuracy assessment provided a useful complementary classification assessment method. In this case, results showed that for objects of classes that varied in

size and shape, such as the shrub class, classification accuracy is highly conditioned by the ground feature size, and thus by the spatial configuration and heterogeneity of classes.

Our results indicate that it is desirable to carry out a per-object assessment with at least one relevant class that has well-delineated boundaries as an accuracy indicator. According to the per-pixel classification assessment methods and conditional kappa statistics, the PAN:MULT and MULT maps were not significantly different. However, the more detailed per-object accuracy assessment revealed that the inclusion of the

**Table 3.** Contingency matrix for the per-object classification assessment for the panchromatic and multispectral layers (PAN:MULT) and the multispectral only (MULT) maps, considering the number of objects and the area as accuracy metrics

	Number of objects				Area (m <sup>2</sup> )			
	Reference data				Reference data			
	Shrubs	Not detected	Total	Correctness	Shrubs	Not detected	Total	Correctness
<i>Classified data</i>								
PAN:MULT								
Shrubs	425	30	455	93.4%	54590.0	8988.4	63578.5	85.9%
Not detected	528		528		16020.8		16020.8	
Total	953	30	983		70610.8	8988.4	79599.3	
Completeness	44.6%				77.3%			
MULT								
Shrubs	130	3	133	97.7%	51597.2	9864.3	61461.5	84.0%
Not detected	876		876		19013.7		19013.7	
Total	1006	3	1009		70610.8	9864.3	80475.1	
Completeness	12.9%				73.1%			

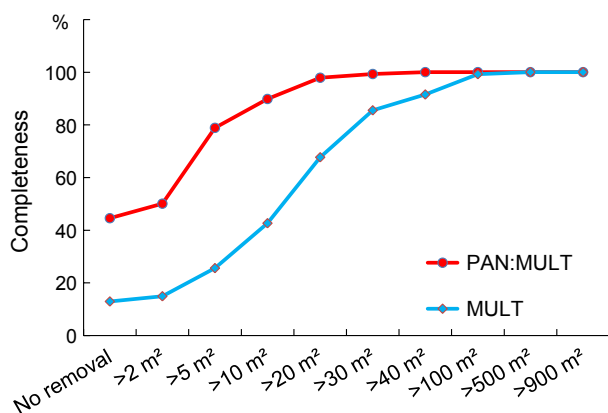


**Fig. 4.** Effect of object size on the completeness accuracy (expressed in number of objects) of objects of the panchromatic and multispectral (PAN:MULT) and the multispectral only (MULT) maps. Reference shrub objects below a given size (between 2 and 900 m<sup>2</sup>) were iteratively removed (*x*-axis). Completeness was calculated as a function of the minimum size of shrub objects retained in the reference sample.

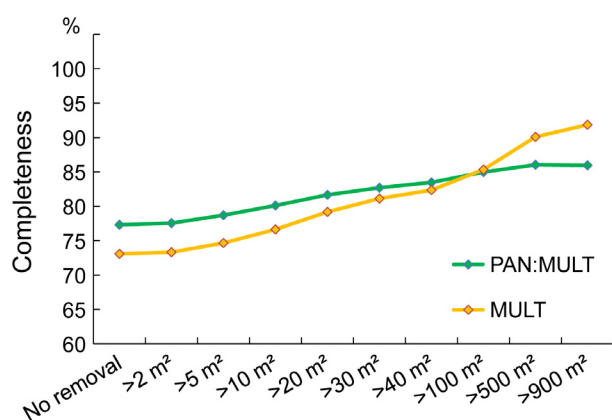


**Fig. 5.** Effect of object size on the completeness accuracy (expressed in object area) classified as shrubs in the panchromatic and multispectral map (PAN:MULT) and the multispectral only (MULT). Reference shrub objects below a given size (between 2 and 900 m<sup>2</sup>) were iteratively removed (*x*-axis). Completeness was calculated as a function of the minimum size of shrub objects retained in the reference sample.

panchromatic layer in the classification process extended the capability of the imagery to identify smaller shrub patches. When considering the number of reference objects detected, there was general low completeness in both maps, that is, many objects were missed, but high correctness values were evident. Consequently, low overall accuracies resulted, based on the grain or pixel size. Completeness increased after systematically removing objects, revealing that many patches <5 m<sup>2</sup> and <30 m<sup>2</sup> were missed in the PAN:MULT and MULT maps, respectively. Hence, the overall low per-object classification accuracies in terms of number of objects are explained by the high level of fragmentation of shrubs in the study area, although these sparse shrubs represent a low total amount of cover. The larger the size of a ground feature, the greater the match between the reference and the classified shrub objects, and the subsequent object classification, with overlapping inaccuracies generally due to over- or under-segmentation (Möller, Lyburner & Volk 2007). Small nearby shrub patches are also likely to be classified within larger objects, implying an over-classification of interstitial spaces.

The inclusion of the panchromatic layer did not affect resource selection models at the chosen scale (20–30 m radius) for the type of variables examined. This suggests that the acquisition of panchromatic imagery may not be required for studies working at this scale and using similar variables, thus reducing project costs. The variability in cover area and configuration captured within the defined buffers produced equivalent top-ranked models using RSF. Therefore, the landscape measures using the two maps are likely to vary only slightly, and thus would not alter the RSA results. Feral cat resource selection was positively influenced by the combination of habitats linked to the presence of rabbits and refugia. Hedgehogs established home ranges in pastoral landscapes containing abundant edges and high vegetation productivity (mainly green pastures and shrubs), which provide food, primarily invertebrates and dry shelter (Recio *et al.* 2013).

The level of detail obtained in this research using the combination of VHSR and OBIA is suitable for use in conjunction with a location error of ±30 m (Recio *et al.* 2011). As noted

**Table 4.** Description of the best models for hedgehogs and feral cats obtained from resource selection functions using Akaike Information Criterion (AIC) for model selection. Landscape cover and metrics were extracted independently from the map produced by combining the panchromatic and multispectral layers (PAN:MULT) or from the multispectral layers only (MULT). Variables were integrated within two independent resource selection analyses (using variables from PAN:MULT and MULT, respectively) as covariates

Species	Variable	PAN:MULT		MULT	
		Coefficient	SE	Coefficient	SE
Hedgehog	Total Edge	0.00026	0.00015	0.00041	0.00003
	NDVI	4.49300	0.1786	5.04700	0.17550
	Distance to roads	−0.00537	0.00007	−0.00053	0.00007
	Distance to tracks	0.00085	0.00005	0.00007	0.00005
Feral cats	Shrubs	0.00391	0.00004	0.03799	0.00004
	Meadow	0.02360	0.00003	0.02529	0.00003
	Elevation	−0.00470	0.00001	−0.00479	0.00006
	Bare ground on slopes	0.01550	0.00008	0.01460	0.00008

earlier, this is generally consistent with results reported for wildlife GPS-devices (Frair *et al.* 2010). The scale discrepancy between the GPS-driven error and the detailed information obtained from the PAN:MULT map may be a possible explanatory factor for the same best models obtained for both maps. However, improvements in GPS accuracy will make it possible to capture better landscape cover and patterns within smaller buffers than those used here, and thus, the incorporation of the panchromatic layer may provide more relevant details. Further tests are also required to assess how variations in map resolution may affect other RSA methods such as RUF, step selection functions or mechanistic models.

Our results suggest that RSA and detailed animal movement research that require information about landscape composition and configuration features can be achieved using the multispectral layers of VHSR satellite images in conjunction with OBIA techniques. The panchromatic layer using Quickbird imagery can be included in the analysis if characterization of ground objects of  $\sim 5 \text{ m}^2$  is required.

Scientists and wildlife managers requiring detailed maps of habitat features need to consider their alternatives carefully in the image pixel sizes offered by commercial satellites, the associated costs in relation to the size of the study area, and the likely benefits of acquiring the relatively more expensive panchromatic imagery to answer their research questions. The techniques used in this research are also applicable to other wildlife spatial ecology applications requiring fine scales, including mapping patterns of biodiversity where, until recently, the spatial resolution of maps has been too coarse to be useful for resource managers (Culbert *et al.* 2012); remote detection of breeding areas of seabirds (Hughes, Martin & Reynolds 2011); and censusing of colonial species (Fretwell *et al.* 2012).

## Acknowledgements

Department of Conservation Twizel for logistic support. Pascal Sirguy for comments on image preprocessing. Research supported by PBRF Grants from the Department of Zoology and the School of Surveying, Otago University, and Ministry of Business Innovation and Employment and Foundation for Research Science and Technology (FRST) Grant UOOX09043. Mariano R. Recio was funded by a PhD scholarship from the University of Otago.

## References

Addink, E.A., de Jong, S.M. & Pebesma, E.J. (2007) The importance of scale in object-based mapping of vegetation parameters with hyperspectral imagery. *Photogrammetric Engineering & Remote Sensing*, **73**, 905–912.

Benz, U., Hofmann, P., Willhauck, G., Lingenfelder, I. & Heynen, M. (2004) Multiresolution, object-oriented fuzzy analysis of remote sensing data for GIS-ready information. *ISPRS Journal of Photogrammetry and Remote Sensing*, **58**, 239–258.

Blaschke, T. (2010) Object based image analysis for remote sensing. *ISPRS International Journal of Photogrammetry and Remote Sensing*, **65**, 2–16.

Boyce, M.S. (2006) Scale for resource selection functions. *Diversity and Distributions*, **12**, 269–276.

Boyce, M.S. & McDonald, L.L. (1999) Relating populations to habitats using resource selection functions. *Trends in Ecology and Evolution*, **14**, 268–272.

Burnham, K.P. & Anderson, D.R. (2002) *Model Selection and Multimodel Inference*. Springer, New York, USA.

Cameron, B., van Heezik, Y., Maloney, R., Seddon, P. & Harraway, J. (2005) Improving predator capture rates: analysis of river margin trap site data in the Waitaki basin, New Zealand. *New Zealand Journal of Ecology*, **29**, 117–128.

Chen, G., Hay, G.J., Castilla, G., St-Onge, B. & Powers, R. (2011) A multiscale geographic object-based image analysis to estimate lidar-measured forest canopy height using Quickbird imagery. *International Journal of Geographical Information Science*, **25**, 877–893.

Chuvieco, E. (2006) *Teledetección Ambiental. La Observación de la Tierra Desde el Espacio*. 2nd edn. Ariel Ciencia, Barcelona.

Congalton, R. (1991) A review of assessing the accuracy of classifications of remotely sensed data. *Remote Sensing of Environment*, **37**, 35–46.

Culbert, P.D., Radeloff, V.C., St-Louis, V., Flather, C.H., Rittenhouse, C.D., Albright, T.P. & Pidgeon, A.M. (2012) Modeling broad-scale patterns of avian species richness across the Midwestern United States with measures of satellite image texture. *Remote Sensing of Environment*, **118**, 140–150.

Definiens (2010) *ECognition Developer 8.0.1. – User Guide*. 1.2.1 edn. Definiens AG, Munich.

Estes, L.D., Reillo, P.R., Mwangi, A.G., Okin, G.S. & Shugart, H.H. (2010) Remote sensing of structural complexity indices for habitat and species distribution modeling. *Remote Sensing of Environment*, **114**, 792–804.

Forester, D.J., Im, H.K. & Rathouz, P.J. (2009) Accounting for animal movement in estimation of resource selection functions: sampling and data analysis. *Ecology*, **90**, 3554–3565.

Frair, J., Fieberg, J., Hebblewhite, M., Cagnacci, F., DeCesare, N. & Pedrotti, L. (2010) Resolving issues of imprecise and habitat-biased locations in ecological analyses using gps telemetry data. *Philosophical Transactions of the Royal Society B: Biological Sciences*, **365**, 2187–2200.

Franklin, S.E. (2010) *Remote Sensing for Biodiversity and Wildlife Management*. McGraw-Hill, New York.

Fretwell, T.J., LaRue, M.A., Paul Morin, P., Kooyman, G.L., Wienecke, B., Ratcliffe, N. *et al.* (2012) An emperor Penguin population estimate: the first global, synoptic survey of a species from space. *PLoS ONE*, **7**, e33751.

Gillies, C. (2001) Advances in New Zealand mammalogy 1990–2000: House cat. *Journal of the Royal Society of New Zealand*, **31**, 205–218.

Hebblewhite, M. & Haydon, D. (2010) Distinguishing technology from biology: A critical review of the use of GPS telemetry data in ecology. *Philosophical Transactions of the Royal Society B: Biological Sciences*, **365**, 2303–2312.

Horning, N., Robinson, J., Sterling, E., Turner, W. & Spector, S. (2010) *Remote Sensing for Ecology and Conservation*. Oxford University Press, Oxford.

Hosmer, D.W. & Lemeshow, S. (2000) *Applied Logistic Regression*. Wiley, New York.

Huete, A. (1988) A soil-adjusted vegetation index (SAVI). *Remote Sensing of Environment*, **25**, 295–309.

Hughes, G.B., Martin, G.R. & Reynolds, S.J. (2011) The use of Google Earth™ satellite imagery to detect the nests of masked boobies *Sula dactylatra*. *Wildlife Biology*, **17**, 210–216.

IUCN (2012) *IUCN Red List of Threatened Species. Version 2012.2*. URL <http://www.iucnredlist.org> [accessed 25 March 2013].

Jones, C. & Norbury, G. (2006) Habitat use as a predictor of nest raiding by individual hedgehogs *Erinaceus europaeus* in New Zealand. *Pacific Conservation Biology*, **12**, 180–188.

Lahoz-Monfort, J.J., Guillera-Arroita, G., Milner-Gulland, E.J., Young, R.P. & Nicholson, E. (2010) Satellite imagery as a single source of predictor variables for habitat suitability modelling: how Landsat can inform the conservation of a critically endangered lemur. *Journal of Applied Ecology*, **47**, 1094–1102.

Laliberte, A., Rango, A., Havstad, K., Paris, J., Beck, R., McNeely, R. & Gonzalez, A. (2004) Object-oriented image analysis for mapping shrub encroachment from 1937 to 2003 in southern New Mexico. *Remote Sensing of Environment*, **93**, 198–210.

Landis, J.R. & Kock, G.G. (1977) The measurement of observer agreement for categorical data. *Biometrics*, **33**, 159–174.

Marzluff, J.M., Millsbaugh, J.J., Hurvitz, P. & Handcock, M.S. (2004) Relating resources to a probabilistic measure of space use: forest fragments and Steller's Jays. *Ecology*, **85**, 1411–1427.

Mathieu, R., Freeman, C. & Aryal, J. (2007) Mapping private gardens in urban areas using object-oriented techniques and very high-resolution satellite imagery. *Landscape and Urban Planning*, **81**, 179–192.

Möller, M., Lymburner, L. & Volk, M. (2007) The comparison index: a tool for assessing the accuracy of image segmentation. *International Journal of Applied Earth Observation and Geoinformation*, **9**, 311–321.

Moorcroft, P.J. & Barnett, A. (2008) Mechanistic home range models and resource selection analysis: a reconciliation and unification. *Ecology*, **89**, 1112–1119.

Mysterud, A. & Ims, R.A. (1998) Functional responses in habitat use: availability influences relative use in trade-off situations. *Ecology*, **88**, 56–62.

Pohl, C. & van Genderen, J. (1998) Multisensor image fusion in remote sensing: concepts, methods and applications. *International Journal of Remote Sensing*, **19**, 823–854.

- Recio, M.R. (2011) *Spatial Ecology of Introduced Mammalian Predators in New Zealand: Using Satellite Technology to Quantify Resource Selection*. PhD thesis, University of Otago, Dunedin.
- Recio, M.R., Mathieu, R., Denys, P., Sirguey, P. & Seddon, P.J. (2011) Lightweight GPS-Tags, one giant leap for wildlife tracking? An Assessment Approach *PLoS ONE*, **6**, e28225.
- Recio, M.R., Mathieu, R., Latham, M.C., Latham, A.D.M. & Seddon, P.J. (2013) Quantifying fine-scale resource selection by introduced European hedgehogs (*Erinaceus europaeus*) in ecologically sensitive areas. *Biological Invasions*, **15**, 1807–1818.
- Richter, R. (1998) Correction of satellite imagery over mountainous terrain. *Applied Optics*, **37**, 4004–4015.
- Rubio, J.L. & Carrascal, L.M. (1994) Habitat selection and conservation of an endemic Spanish lizard (*Algyroides marchi*) (Reptilia, Lacertidae). *Biological Conservation*, **70**, 245–250.
- Skidmore, A. (1999). Accuracy assessment of spatial information. *Spatial Statistics for Remote Sensing* (eds. A. Stein, F. van der Meer & B. Gorte), pp. 197–209. Kluwer Academic Publishers, Dordrecht.
- Toutin, T. (2004) Geometric processing of remote sensing images: models, algorithms and methods. *International Journal of Remote Sensing*, **25**, 1893–1924.
- Tucker, C.J. (1979) Red and photographic infrared linear combinations for monitoring vegetation. *Remote Sensing of the Environment*, **8**, 127–150.
- Zhan, Q., Martien, M., Tempfli, L. & Shi, W. (2005) Quality assessment for geospatial objects derived from remotely sensed data. *International Journal of Remote Sensing*, **26**, 2953–2974.

Received 27 March 2013; accepted 8 July 2013

Handling Editor: Darren Kriticos

## Supporting Information

Additional Supporting Information may be found in the online version of this article.

**Table S1.** Parameters selected in eCognition software for panchromatic and multispectral (PAN:MULT) and multispectral (MULT) segmentation.

**Table S2.** Selected land-cover classes for Godley Valley.

**Table S3.** Error matrix for the per-pixel assessment of the panchromatic and multispectral (PAN:MULT) classification.

**Table S4.** Error matrix for the per-pixel assessment of the multispectral only (MULT) classification.